

Glutaraldehyde Crosslinked Alginate-Chitosan Nanoparticles as Paracetamol Adsorbent

Nurmala Nurmala, Adhitasari Suratman*, and Suherman Suherman

Department of Chemistry, Faculty of Mathematics and Natural Sciences, Universitas Gadjah Mada, Sekip Utara, Yogyakarta 55281, Indonesia

* **Corresponding author:**

email: adhitasari@ugm.ac.id

Received: February 19, 2023

Accepted: September 11, 2023

DOI: 10.22146/ijc.82431

Abstract: Paracetamol contained in wastewater can cause adverse effects on animal ecosystems, such as fish living in waters and cause harmful effects on humans. Adsorption techniques are used to remove these pharmaceutical compounds. Alginate-chitosan nanoparticles are non-toxic and effectively used as adsorbents to remove pharmaceutical compounds in wastewater. Research on glutaraldehyde crosslinked alginate-chitosan nanoparticles as paracetamol adsorbent has been carried out. This research used the ionic gelation method. Nanoparticles were characterized using transmission electron microscopy (TEM), scanning electron microscope (SEM-EDX) and Fourier transform infra-red spectrophotometer (FTIR). Furthermore, the nanoparticles were used for paracetamol adsorption. The results showed that the form nanoparticles are coarse solid powder and brownish yellow. The TEM image shows an average nanoparticle size of 8.22 nm. Glutaraldehyde crosslinked alginate-chitosan nanoparticles adsorbed paracetamol with adsorption kinetics followed a pseudo-second-order or Ho-McKay model, the adsorption rate constant of $0.0324 \text{ g mg}^{-1} \text{ min}^{-1}$. The isotherm study of paracetamol adsorption by glutaraldehyde cross-linked alginate-chitosan nanoparticles followed the isotherm Dubinin-Radushkevich isotherm model with a free energy value of $707.1068 \text{ kJ mol}^{-1}$, and this value indicates the adsorption process by chemically or chemisorption.

Keywords: adsorption; alginate; chitosan; glutaraldehyde; paracetamol

■ INTRODUCTION

Pharmaceutical waste has increased in recent years due to the COVID-19 pandemic, and the drugs used increased more than 2.5 times [1]. The main contaminants found in wastewater are pharmaceutical compounds including antibiotic, analgesic, and antipyretic [2]. Paracetamol is one of the analgesic and antipyretic pharmaceutical compounds often used for medical practice and consumed for human health [3]. Based on reports, paracetamol will be excreted from the body by 58–68% after consumption and then will be released into the wastewater system [4]. High concentrations of paracetamol were detected in Indonesian coastal waters, specifically in Jakarta Bay, namely Angke (610 ng/L) and Ancol (420 ng/L) [5]. High concentrations of paracetamol in wastewater can cause

dangerous diseases in humans, such as liver failure, gastrointestinal, and hepatotoxicity [6]. Paracetamol is non-biodegradable and easily accumulates in the aquatic environment, which can have adverse effects on human health and other living things [7]. Therefore, there must be an effort to overcome the problem of wastewater from pharmaceutical compounds such as paracetamol.

The advantages of separating pharmaceutical compounds using adsorption techniques are easy processing, low cost, high efficiency, and can be regenerated [8]. Nanoparticles can be used as an efficient adsorbent for the removal of pharmaceutical compounds in wastewater; nanoparticles have a small size, large surface area and many active binding sites, which can increase the adsorption capacity [2]. Polysaccharide-based materials can be used to

synthesize nanoparticles and as adsorbents, including chitosan and sodium alginate. Chitosan provides an advantage in the adsorption process because it has amino and hydroxyl groups as active groups and is able to interact with pharmaceutical compounds, phenols, metals, pesticides, and other compounds contained in wastewater [9]. Modifications are required for the synthesis of nanoparticles from chitosan because chitosan is very sensitive to pH and has low thermal stability [10].

Chitosan can be modified by combining certain polymers and crosslinkers to improve the stability and adsorption capacity of chitosan [11]. Alginate is an anionic polymer, that has non-toxic, biodegradable, biocompatible properties, and the anionic properties of alginate can interact with the cationic properties of chitosan to form more stable nanoparticles [11]. Ferrah et al. [12] reported chitosan combined with alginate and polyethyleneimine methylene phosphonic acid to be able to be a promising and efficient adsorbent for removing the pharmaceutical compounds sodium diclofenac and ibuprofen from wastewater.

Chitosan also requires certain crosslinkers for the synthesis of chitosan-based nanoparticles to improve adsorption capacity [4]. Glutaraldehyde is a chitosan crosslinker that can improve the chemical stability of chitosan in acidic solutions and adsorption performance [13]. Kyzas et al. [14] reported chitosan was modified and cross-linked with glutaraldehyde and combined with sulfonate group or *N*-(2-carboxybenzyl) was able to remove pramipexole dihydrochloride, a pharmaceutical compound used to treat symptoms of Parkinson's disease and as a pharmaceutical compound in wastewater. Based on the background, it is necessary to conduct research using polysaccharide-based nanoparticles, such as chitosan and alginate, to remove pharmaceutical compounds such as paracetamol in wastewater.

■ EXPERIMENTAL SECTION

Materials

The materials used in this study came from Merck and Sigma Aldrich with pro analytical quality. These materials include chitosan (Deacetylation Degree $\geq 85\%$), sodium alginate, glutaraldehyde, CaCl_2 , aquabidest, 10%

(v/v) methanol solution, 1% (v/v) acetic acid solution, sodium hydroxide (NaOH), hydrochloric acid (HCl), and paracetamol from pharma grade.

Instrumentation

The instruments used in this study include laboratory glassware, analytical balance, pH meter, magnetic stirrer, hot plate, centrifugation (Sorvall Biofuge Primo), Fourier transform infra-red spectrophotometer (FTIR, Shimadzu Prestige-21) was observed in the absorption range of $400\text{--}4000\text{ cm}^{-1}$. Samples were prepared in a powder state, molded with KBr, and then pressed to form pellets. Nanoparticle size was characterized using transmission electron microscopy (TEM, JEM-1400 JEOL/EO) on a scale of 20–500 nm. Samples were prepared and then characterized. The morphology of the nanoparticles was characterized using a scanning electron microscope (SEM-EDX, JSM-6510 JEOL/EO). The sample was glued to the specimen holder, and then the sample was characterized with the specifications of voltage = 15 kV and magnification of 500–10,000 times. The concentration of paracetamol solution before and after adsorption was determined at 200–400 nm absorption using a UV-vis spectrophotometer (GENESYS 50 Thermo Scientific).

Procedure

Synthesis of glutaraldehyde cross-linked alginate-chitosan nanoparticles

Sodium alginate (3 mg/mL) and CaCl_2 (3.35 mg/mL) solutions were prepared by dissolving in aquabidest. Chitosan was prepared at 3 mg/mL concentration, dissolved in 1% (v/v) acetic acid. 0.1 M HCl solution and 0.1 M NaOH solution were used to adjust the pH of alginate and chitosan solutions to pH 5. Synthesis of glutaraldehyde crosslinked alginate-chitosan nanoparticles was prepared according to Rajaonarivony method with modifications [15]. Calcium alginate (Ca-Alg) in the pre-gel phase was initially prepared by adding 2 mL of CaCl_2 to 10 mL of sodium alginate solution with continuous stirring for 30 min. After that, 10 mL of chitosan solution was added, and then 5 mL of glutaraldehyde was added to the solution while still stirring at constant speed at room

temperature. Stirring process was carried out for 2 h, then centrifuged at 5,000 rpm for 30 min. Nanoparticles were filtered using filter paper and then dried.

Characterization of glutaraldehyde crosslinked alginate-chitosan nanoparticles

Glutaraldehyde crosslinked alginate-chitosan nanoparticles were characterized using a FTIR. The sample was prepared in a powder state, then formed with KBr and pressed to form pellets. FTIR spectra were determined at a wavenumber between 400–4000 cm^{-1} . The size of glutaraldehyde crosslinked alginate-chitosan nanoparticles was characterized using TEM on a scale of 20–500 nm. The samples were dispersed and placed in the grid. The samples in the grid were waited until dry, and the samples were ready for characterization. The morphology of glutaraldehyde crosslinked alginate-chitosan nanoparticles was characterized by SEM. The samples were attached to the specimen holder, and then the samples were ready for characterization with a voltage specification of 15 kV and magnification of 500–10,000 times.

Effect of pH on paracetamol adsorption

Paracetamol solution 10 mg/L, volume of 50 mL was adjusted to pH 2, 3, 4, 5, 6, 7, and 8 with the addition of HCl or NaOH solutions. Glutaraldehyde crosslinked alginate-chitosan nanoparticles adsorbent (20 mg) was added to each paracetamol solution for adsorption. The stirring process was carried out for 60 min, and then the filtrate was filtered. The concentration of paracetamol was analyzed with a UV-vis spectrophotometer at the maximum wavelength (λ_{max}).

Effect of adsorbent mass on paracetamol adsorption

Paracetamol solution 10 mg/L, volume of 50 mL in 9 different containers adjusted to the optimum pH by adding HCl or NaOH solution. Glutaraldehyde crosslinked alginate-chitosan nanoparticles were added to paracetamol solution for the adsorption process with mass variations of 5, 10, 15, 20, 25, 30, 35, and 40 mg and stirred for 60 min then the filtrate was filtered. The concentration of paracetamol was analyzed with a UV-vis spectrophotometer at λ_{max} .

Effect of contact time on paracetamol adsorption

Paracetamol solution 10 mg/L, volume of 50 mL in 7 different containers adjusted to the optimum pH by adding HCl or NaOH solution. Glutaraldehyde crosslinked alginate-chitosan nanoparticles were added to paracetamol solution for the adsorption process at the optimum mass and stirred at various times of 15, 30, 45, 60, 90, and 120 min, then the filtrate was filtered. The concentration of paracetamol was analyzed with a UV-vis spectrophotometer at λ_{max} . The adsorption capacity can be used to determine the adsorption kinetics model.

Effect of initial concentration of paracetamol

Paracetamol solutions are prepared with various concentrations of 10, 12, 14, 16, and 18 mg/L. Paracetamol solution 50 mL in 10 different containers was adjusted to the optimum pH by adding HCl or NaOH solutions. Paracetamol solutions of varying concentrations were prepared for control (without adsorbent) and adsorption (with adsorbent). Glutaraldehyde crosslinked alginate-chitosan nanoparticles were added to the paracetamol solution at optimum mass. The stirring process was carried out according to the optimum contact time, and then the filtrate was filtered. The concentration of paracetamol was analyzed by UV-vis spectrophotometer at λ_{max} .

■ RESULTS AND DISCUSSION

FTIR Characterization

The identification of functional groups in the base material and the synthesized nanoparticles was carried out using an FTIR spectrophotometer. The results of the FTIR spectra of alginate, chitosan, glutaraldehyde, and glutaraldehyde crosslinked alginate-chitosan nanoparticles can be seen in Fig. 1. Fig. 1(a) shows characteristic peaks at 3448, 1410, 1620 and 1026 cm^{-1} which shows stretching vibration –OH, symmetric and asymmetric stretching vibration C=O and stretching vibration C–O–C of alginate [16-18]. Fig. 1(b) shows characteristic peaks at 3450, 1647, 1419 and 1028 cm^{-1} , which shows the stretching of the –NH and –OH groups, the primary amine (–NH₂) bending vibration, –CH₂ and C–O–C stretching vibrations of chitosan [19-21].

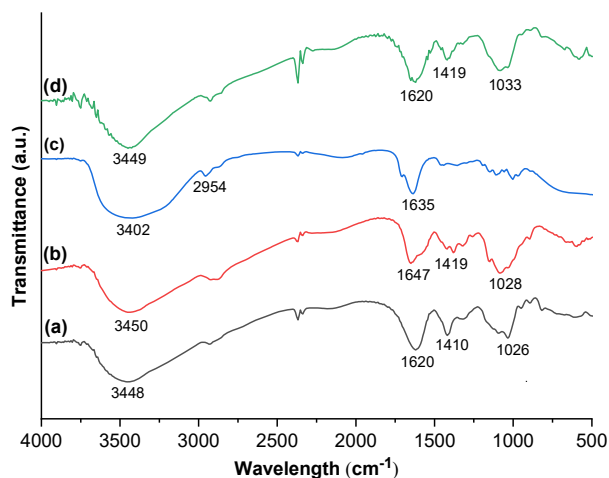


Fig 1. FTIR spectra of (a) alginate, (b) chitosan, (c) glutaraldehyde, and (d) glutaraldehyde crosslinked alginate-chitosan nanoparticles

Fig. 1(c) shows characteristic peaks at 3402, 2954, and 1635 cm^{-1} , which shows $-\text{OH}$ stretching vibrations, symmetric $\text{C}-\text{H}$ vibrations, and $\text{C}=\text{O}$ stretching vibrations of glutaraldehyde [22]. Fig. 1(d) shows the alginate peak at 3448 cm^{-1} , indicating the presence of $-\text{OH}$ stretching vibrations, and chitosan peaks at 3450 cm^{-1} , indicating the stretching vibrations of $-\text{OH}$ and $-\text{NH}$, shifted the wavenumber to 3449 cm^{-1} . This shift occurs due to electrostatic interactions between the

carboxylic groups from alginate and the amine groups from chitosan to form a polyelectrolyte complex [23]. The chitosan peak at 1647 cm^{-1} wavelength, the alginate peak at 1620 cm^{-1} and the glutaraldehyde peak at 1635 cm^{-1} shifted to 1620 cm^{-1} wavelength, indicating the presence of $-\text{NH}$ bending vibrations from chitosan and $\text{C}=\text{O}$ asymmetric stretching vibrations from alginate and indicating the $\text{C}=\text{O}$ group in glutaraldehyde interacts with the amine groups in chitosan to form $\text{C}=\text{N}$ bonds (imines) [24]. Furthermore, there was a shift in 1419 cm^{-1} wavelength from the alginate peak at 1410 cm^{-1} and chitosan at 1405 cm^{-1} , indicating the presence of $-\text{CH}_2$ bending vibrations from chitosan and $\text{C}=\text{O}$ symmetrical stretching vibrations from alginate. Then, 1028 cm^{-1} of chitosan and 1026 cm^{-1} of alginate shifts to 1033 cm^{-1} wavelength indicating the presence of $\text{C}-\text{O}-\text{C}$ stretching vibrations.

SEM-EDX Characterization

The surface morphology and elemental composition of glutaraldehyde cross-linked alginate-chitosan nanoparticles are determined by using SEM-EDX before and after adsorption. SEM images taken at 5000 times magnification of the nanoparticles before and after adsorption can be seen in Fig. 2. Fig. 2(a) shows

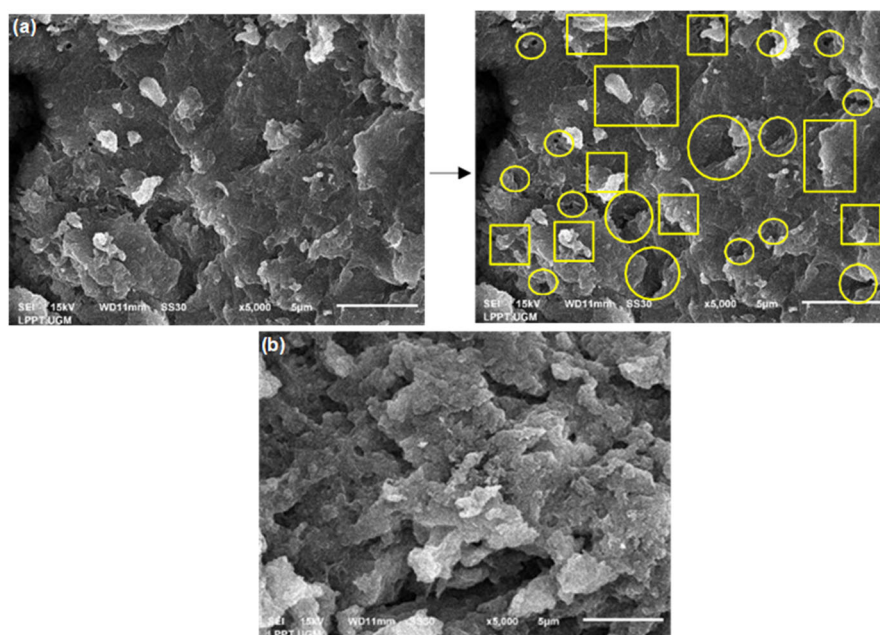


Fig 2. SEM image (a) glutaraldehyde crosslinked alginate-chitosan nanoparticles before adsorption and (b) glutaraldehyde crosslinked alginate-chitosan nanoparticles after adsorption

the nanoparticles before adsorption have a rough, irregular, slightly porous surface, and there are parts that form aggregates. There is a difference between the nanoparticles after and before adsorption in Fig. 2(b); the loss of the porous structure in the SEM image of the nanoparticles after adsorption is possible because the surface of the adsorbent has been covered by paracetamol. The elemental composition data of alginate-chitosan nanoparticles crosslinked with glutaraldehyde before adsorption and after adsorption can be seen in Table 1.

The adsorption process on glutaraldehyde crosslinked alginate-chitosan nanoparticles can be seen from changes in the elemental composition of nanoparticles before and after adsorption. The composition of C and O elements in nanoparticles has increased, as can be seen in Table 1. The C element has a weight and atomic percentage of 37.41 and 43.98%; after adsorption, the percentage of weight and atomic increases to 38.79 and 45.01%. Then, the weight and atomic percentage of O elements were 43.85 and 38.70%, after adsorption increased to 45.92 and 40.00%. Increasing the composition of C and O elements, which are the elemental composition of paracetamol indicates paracetamol was adsorbed on glutaraldehyde crosslinked alginate-chitosan nanoparticles.

TEM Characterization

Nanoparticle characterization using TEM was carried out to determine the inner morphology and average size of the nanoparticles. The results of the characterization of glutaraldehyde crosslinked alginate-chitosan nanoparticles by TEM at a magnification scale of

50 nm are shown in Fig. 3. Based on Fig. 3(a), the TEM image of the nanoparticles has a shape like black spheres but relatively irregular. The graph of the particle size distribution of nanoparticles can be seen in Fig. 3(b). The glutaraldehyde crosslinked alginate-chitosan nanoparticles sample has an average particle size of 8.22 nm. This indicates the ionic gelation method is able to produce smaller particle sizes.

Effect of pH

Based on Fig. 4(a), the adsorption capacity in adsorbing paracetamol has the highest value at pH 4, which is 18.64 mg/g. As the pH of the solution increases, the adsorption capacity value decreases. Fig. 4(b) is a pH point of zero charges (pH_{pzc}) glutaraldehyde crosslinked alginate-chitosan nanoparticle adsorbent. The pH_{pzc} curve shows the intersection at pH 4.773; at that pH, the nanoparticles adsorbent has an uncharged structure. The nanoparticle adsorbent has a positively charged structure when the pH solution is below pH_{pzc} ($pH < 4.773$), while the pH solution is above pH_{pzc} ($pH > 4.773$). Glutaraldehyde crosslinked alginate-chitosan nanoparticles adsorbent has a negatively charged structure.

Based on Fig. 4(a), increasing adsorption capacity occurs at pH 2–4 because the positively charged nanoparticles adsorbent resulted in an electrostatic attraction force with a negative charge on paracetamol. While, decreasing adsorption capacity occurs at pH 5–8 because the nanoparticles adsorbent is negatively charged, and as the pH increases, paracetamol becomes ionized and negatively charged, resulting in a repulsive force between the adsorbent and the adsorbent [25-26].

Table 1. Elemental composition data of glutaraldehyde crosslinked alginate-chitosan nanoparticles before and after adsorption

| Element | Weight % | | Atom % | |
|---------|-------------------|------------------|-------------------|------------------|
| | Before adsorption | After adsorption | Before adsorption | After adsorption |
| C | 37.41 | 38.79 | 43.98 | 45.01 |
| N | 15.67 | 14.92 | 15.80 | 14.85 |
| O | 43.85 | 45.92 | 38.70 | 40.00 |
| Na | 1.58 | 0.05 | 0.97 | 0.03 |
| Cl | 0.61 | 0.10 | 0.24 | 0.04 |
| Ca | 0.89 | 0.22 | 0.31 | 0.08 |

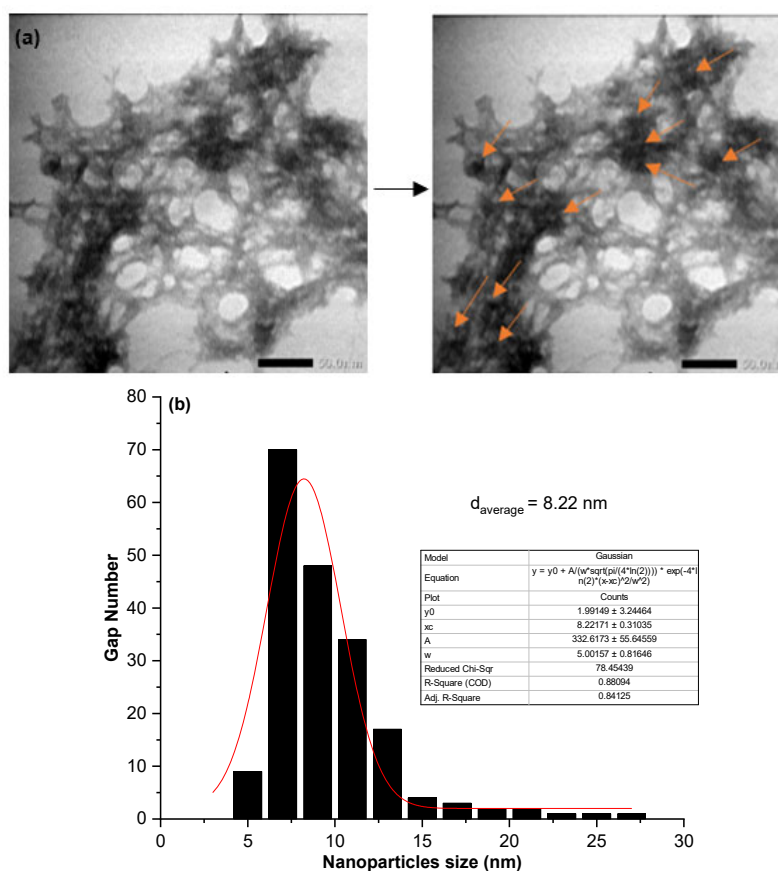


Fig 3. (a) TEM image of glutaraldehyde crosslinked alginate-chitosan nanoparticles, (b) Particle size distribution of glutaraldehyde crosslinked alginate-chitosan nanoparticles

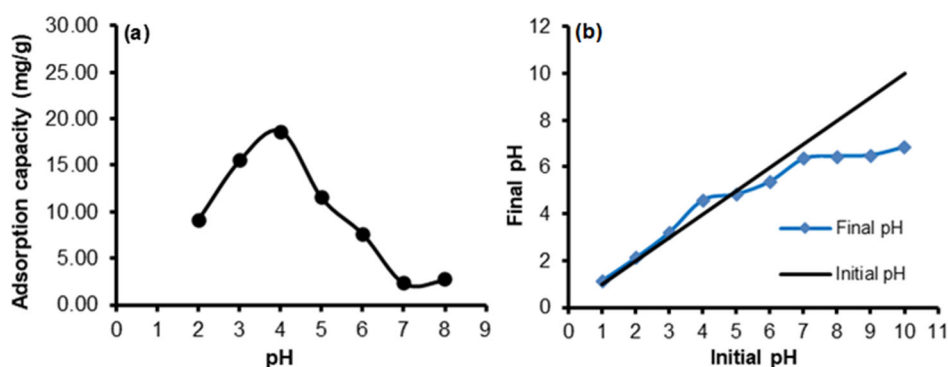


Fig 4. (a) Effect of pH on paracetamol adsorption by glutaraldehyde crosslinked alginate-chitosan nanoparticles adsorbent and (b) pH curve point of zero charge (pH_{pzc}) glutaraldehyde crosslinked alginate-chitosan nanoparticles adsorbent

Effect of Adsorbent Mass

Fig. 5 shows the effect of adsorbent mass on the mass of paracetamol adsorbed by glutaraldehyde crosslinked alginate-chitosan nanoparticles, the optimum point at 30 mg adsorbent mass. The mass of paracetamol obtained

was 0.3501 mg at the optimum mass point of the adsorption process. The mass of paracetamol adsorbed by the nanoparticles will also increase as the adsorbent mass increases. This increase was related to the number of active sites and the surface area of the adsorbent. The

greater the mass of the adsorbent, the greater the surface area, causing more opportunities for contact or interaction between the adsorbent and adsorbate. Based on Fig. 5, decreasing the mass of paracetamol adsorbed by nanoparticles occurs when the adsorbent mass is greater than 30 mg. The equilibrium of the adsorption process occurs when the adsorbed paracetamol has reached the optimum point, so the addition of the amount of adsorbent will disturb the equilibrium [27].

Effect of Contact Time

Fig. 6 shows the equilibrium adsorption of paracetamol by nanoparticles with the largest adsorption capacity of 10.06 mg/g obtained at 45 min. Then, the adsorption capacity of paracetamol decreased after the optimum contact time. This is because after reaching an equilibrium state, the adsorbent becomes saturated so that the active site is no longer able to interact with the adsorbate. In this research, the study of adsorption on the effect of contact time was used to determine the kinetic model of paracetamol adsorption by glutaraldehyde crosslinked alginate-chitosan nanoparticles. The adsorption kinetics models used are pseudo-first-order kinetic models and pseudo-second-order kinetic models. The pseudo-first-order kinetic model is expressed by Eq. (1);

$$\ln(q_e - q_t) = \ln q_e - k_1 t \quad (1)$$

where q_e (mg g^{-1}) is the adsorption capacity at equilibrium, q_t (mg g^{-1}) is the adsorption capacity at time t (min), k_1 (min^{-1}) is the pseudo-first-order rate constant.

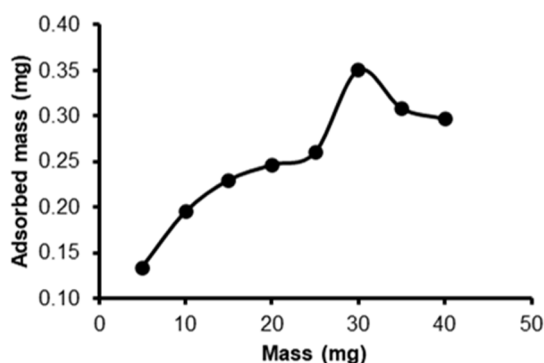


Fig 5. Effect of adsorbent mass on the mass of paracetamol adsorbed by glutaraldehyde crosslinked alginate-chitosan nanoparticles

The graph of the sum of $\ln(q_e - q_t)$ against time can determine the value of q_e from the intercept and k_1 from the slope [27]. The pseudo-second-order kinetic model is expressed by Eq. (2).

$$\frac{t}{q_t} = \left(\frac{1}{k_2 q_e^2} \right) + \frac{1}{q_e} t \quad (2)$$

In Eq. (2), q_e (mg g^{-1}) is the adsorption capacity at equilibrium, q_t (mg g^{-1}) is the adsorption capacity at a certain t (min), k_2 ($\text{g mg}^{-1} \text{min}^{-1}$) is the pseudo-second-order adsorption rate constant. A linear graph of $\frac{t}{q_t}$ against time can determine the value of q_e from the slope and k_2 from the intercept [28].

The linear graphs of the two adsorption kinetics models used are shown in Fig. 7, and the adsorption kinetics parameter values of the two adsorption kinetics models are presented in Table 2. The kinetic model has a linearity value (R^2) close to 1, is the pseudo-second-order kinetics model or the Ho-McKay model, which is equal to 0.9993 and the line equation obtained is $y = 0.097x + 0.2908$ in Fig. 7. The linearity value indicates the adsorption of paracetamol by nanoparticles following the pseudo-second-order kinetic model. In Table 2, the pseudo-second-order kinetic model obtained the value of the adsorption rate constant (k) of $0.0324 \text{ g mg}^{-1} \text{min}^{-1}$ and adsorption capacity value (q_e) of $10.3093 \text{ mg g}^{-1}$. The pseudo-second-order kinetic model assumes the chemisorption process occurs at the determination of the adsorption rate [29]. The adsorption rate is not influenced by the adsorbate

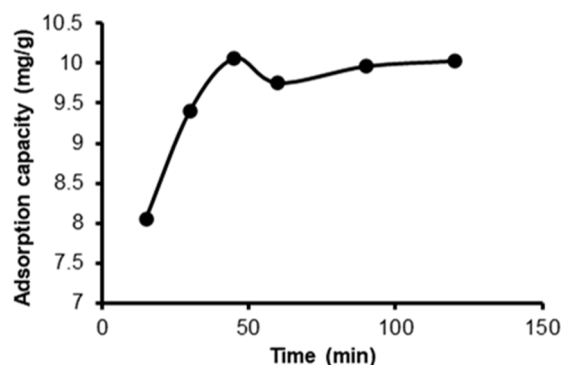


Fig 6. Effect of contact time on paracetamol adsorption by glutaraldehyde crosslinked alginate-chitosan nanoparticle

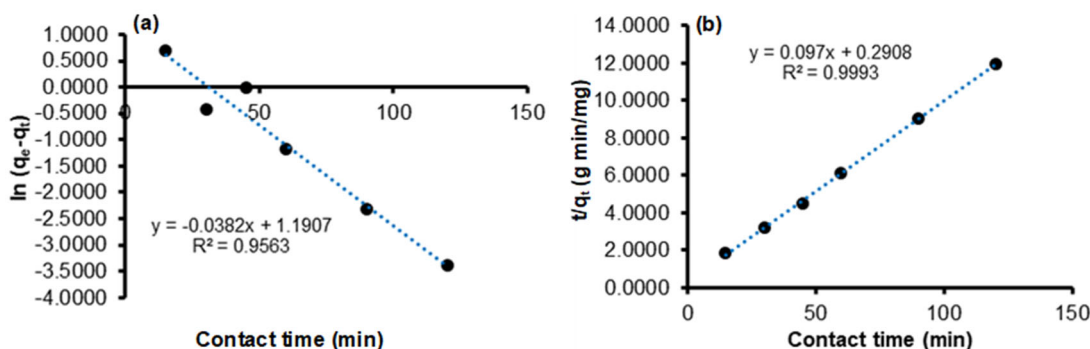


Fig 7. Plot of adsorption kinetics model (a) pseudo-first-order and (b) pseudo-second-order models on the adsorption process of paracetamol by glutaraldehyde crosslinked alginate-chitosan nanoparticles

Table 2. The parameter calculation result of pseudo-first-order and pseudo-second-order models

| Model | Parameter | Score |
|---------------------------------------|--|---------|
| Pseudo-first-order or Lagergren model | R^2 | 0.9563 |
| | k (min^{-1}) | 0.0382 |
| | q_e (mg/g) | 3.2894 |
| Pseudo-second-order or Ho-McKay model | R^2 | 0.9993 |
| | k ($\text{g mg}^{-1} \text{min}^{-1}$) | 0.0324 |
| | q_e (mg/g) | 10.3093 |

concentration but is influenced by the adsorption capacity at these conditions [30].

Effect of Initial Concentration

Fig. 8 shows the equilibrium condition for paracetamol adsorption by glutaraldehyde crosslinked alginate-chitosan nanoparticles was reached at an initial paracetamol concentration of 16 ppm, and the largest adsorption capacity was 14.3396 mg/g. The adsorption capacity of paracetamol decreased after the optimum condition was reached. The number of adsorbate active sites in the solution is greater due to the greater initial concentration of paracetamol. Meanwhile, the constant mass of the adsorbent causes the number of active sites available on the adsorbent to also remain constant, so when passing through the optimum conditions with a larger initial paracetamol concentration, the amount of adsorbate in solution with the number of particles and the available active sites of the adsorbent becomes unbalanced.

The adsorption capacity obtained will decrease because saturation conditions have been reached [31]. The study of the effect of the initial concentration of

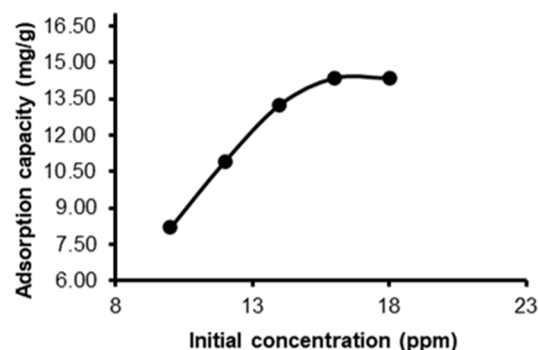


Fig 8. Effect of initial concentration on paracetamol adsorption by glutaraldehyde crosslinked alginate-chitosan nanoparticles

paracetamol will be able to also determine the adsorption isotherm of paracetamol by nanoparticles. The adsorption isotherm in this study was studied using four adsorption isotherm models: Langmuir, Freundlich, Temkin, and Dubinin-Radushkevich isotherm models. The Langmuir isotherm model can be expressed in Eq. (3);

$$\frac{C_e}{q_e} = \frac{1}{k_L q_m} + \frac{C_e}{q_m} \quad (3)$$

where q_m (mg g^{-1}) is the maximum monolayer adsorption capacity, k_L (L mol^{-1}) is the maximum monolayer adsorption capacity, q_e (mg g^{-1}) is the adsorption capacity at equilibrium, and C_e (mol L^{-1}) is the adsorbate concentration at equilibrium. A linear graph between $\frac{C_e}{q_e}$ against C_e can determine the value of q_m from the slope and the value of k_L from the intercept [32]. The Freundlich isotherm model can be expressed in Eq. (4);

$$\log q_e = \log k_F + \frac{1}{n} \log C_e \quad (4)$$

where k_F ($L \text{ mol}^{-1}$) is the Freundlich constant, $\frac{1}{n}$ is the adsorption intensity, q_e (mg g^{-1}) is the adsorption capacity at equilibrium, and C_e (mol L^{-1}) is the adsorbate concentration at equilibrium. $\frac{1}{n}$ value of the slope and k_F value of the intercept can be determined by making a linear graph of $\log q_e$ against $\log C_e$. The Temkin isotherm model can be expressed in Eq. (5);

$$q_e = \frac{RT}{b} \ln(k_T) + \frac{RT}{b} \ln(C_e) \quad (5)$$

where k_T ($L \text{ mol}^{-1}$) is the equilibrium binding constant, b is the heat of adsorption, R is the gas constant ($8.314 \text{ J K}^{-1} \text{ mol}^{-1}$), T (K) is the temperature, q_e (mg g^{-1}) is the adsorption capacity at equilibrium, and C_e (mol L^{-1}) is the adsorbate concentration at equilibrium. A linear graph between q_e and $\ln(C_e)$ will give a straight line with $\frac{RT}{b}$ as the slope and $\frac{RT \ln(k_T)}{b}$ as the intercept [32]. The Dubinin Radushkevich (D-R) isotherm model can be expressed in Eq. (6);

$$\ln q_e = \ln q_m - \beta \varepsilon^2 \quad (6)$$

where q_e (mg g^{-1}) is the adsorption capacity at equilibrium, q_m (mg g^{-1}) is the theoretical isotherm saturation capacity, β ($\text{mol}^2 \text{ J}^{-2}$) is the adsorption energy constant, and ε (J mol^{-1}) is the Polanyi potential. Polanyi potential can be calculated in Eq. (7);

$$\varepsilon = RT \ln \left(1 + \frac{1}{C_e} \right) \quad (7)$$

where T (K) is the temperature, R is the gas constant ($8.314 \text{ J K}^{-1} \text{ mol}^{-1}$), and C_e (mg L^{-1}) is the concentration of adsorbate solution in the adsorbent at equilibrium. A linear graph between $\ln q_e$ and ε^2 can determine the β value from the slope and the q_e value from the intercept. The β value will give the average adsorption free energy (E , kJ mol^{-1}) per adsorbate molecule at the time of its transfer to the surface of the solid from the solution, following Eq. (8) [32].

$$E = \frac{1}{(2\beta)^{1/2}} \quad (8)$$

The linear graph of the adsorption isotherm model is shown in Fig. 9, and Table 3 is a summary of the parameter calculation results for each paracetamol adsorption isotherm model by nanoparticles. Fig. 9 shows the plot of the adsorption isotherm model. Fig. 9(d) is the

Dubinin-Radushkevich isotherm model having a linearity value (R^2) closest to 1, equal to 0.9819 and the equation of the line is $y = -1 \times 10^{-6}x + 2.8629$. Based on this, the adsorption of paracetamol by nanoparticles follows the Dubinin-Radushkevich isotherm model. In Table 3, the Dubinin-Radushkevich isotherm model has a value of q_e of $17.5122 \text{ mg g}^{-1}$. The value of adsorption energy (E) is $707.1068 \text{ kJ mol}^{-1}$.

Based on the adsorption energy (E) value obtained of $707.1068 \text{ kJ mol}^{-1}$, it shows the adsorption of paracetamol by glutaraldehyde crosslinked alginate-chitosan nanoparticles occurs through a chemical adsorption process. This is because the E value obtained has a value greater than 16 kJ mol^{-1} . This is in accordance with the statement on the Dubinin-Radushkevich isotherm model that the type of adsorption on the experimental results is chemical adsorption if the E value has a value greater than 16 kJ mol^{-1} [33].

Possible interactions between paracetamol and glutaraldehyde crosslinked alginate-chitosan nanoparticles include hydrogen bonds between N atoms on the adsorbent and H atoms on paracetamol, H atoms on the adsorbent and O atoms on paracetamol, and $n-\pi$ bonds between the adsorbent and adsorbate (Fig. 10).

Table 3. Parameter calculation results for paracetamol adsorption isotherm models by glutaraldehyde crosslinked alginate-chitosan nanoparticles

| Model and parameter | Score |
|-------------------------------------|------------|
| Langmuir isotherm | |
| R^2 | 0.7954 |
| k_L ($L \text{ mol}^{-1}$) | 0.1680 |
| q_m (mg g^{-1}) | 31.1526 |
| Freundlich isotherm | |
| R^2 | 0.9047 |
| k_F ($L \text{ mol}^{-1}$) | 4.9477 |
| N | 1.5038 |
| Temkin isotherm | |
| R^2 | 0.9229 |
| k_T ($L \text{ mol}^{-1}$) | 4.5563 |
| B | 19964.3191 |
| Dubinin-Radushkevich (D-R) isotherm | |
| R^2 | 0.9819 |
| q_e (mg g^{-1}) | 17.5122 |
| E (kJ mol^{-1}) | 707.1068 |

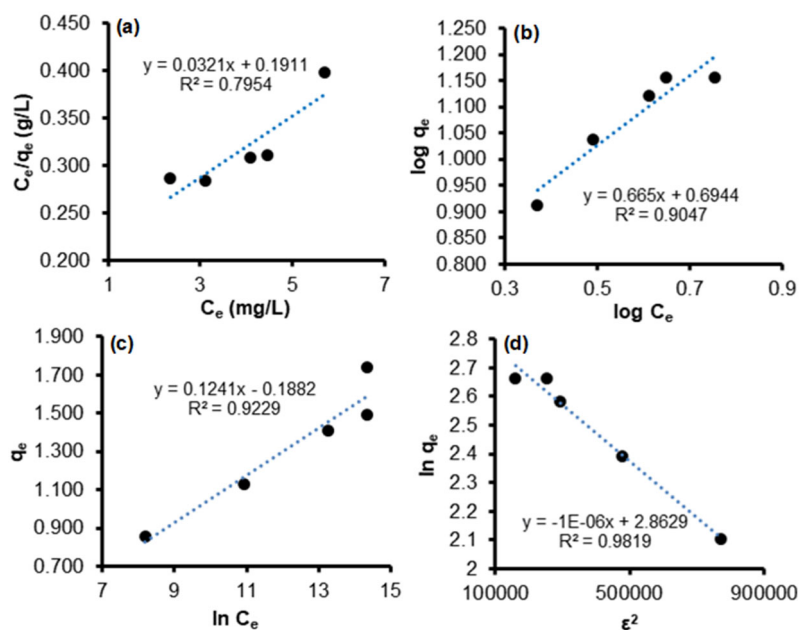


Fig 9. Plot of adsorption isotherm models: (a) Langmuir isotherm, (b) Freundlich isotherm, (c) Temkin isotherm, and (d) Dubinin-Radushkevich isotherm on paracetamol adsorption process by glutaraldehyde crosslinked alginate-chitosan nanoparticles

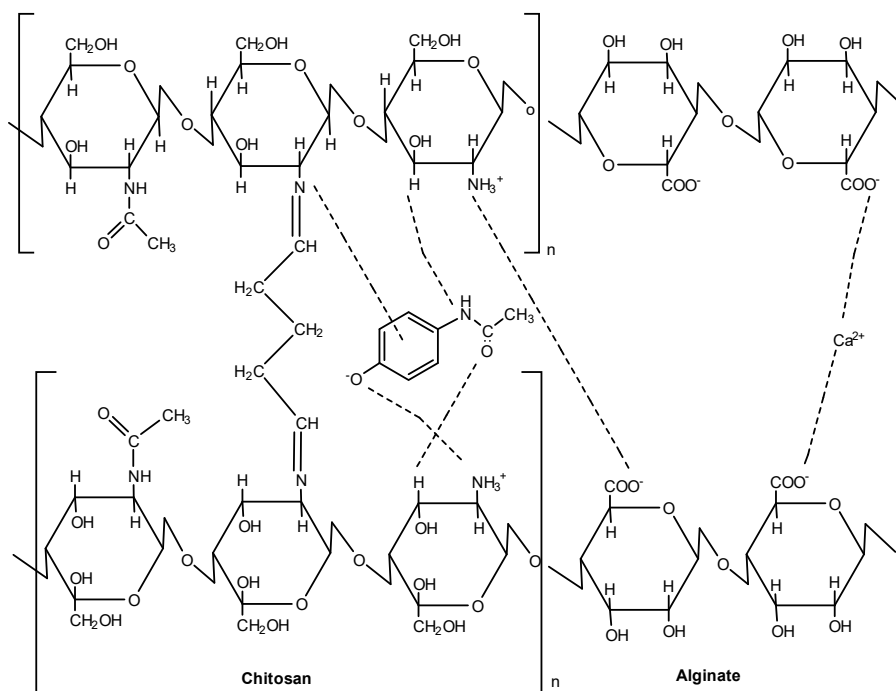


Fig 10. Possible interactions between paracetamol and glutaraldehyde crosslinked alginate-chitosan nanoparticles

■ CONCLUSION

Glutaraldehyde crosslinked alginate-chitosan nanoparticles were successfully synthesized using the ionic gelation method. The nanoparticles have an average

particle size of 8.22 nm. Optimum conditions for paracetamol adsorption by nanoparticles were obtained at pH 4, adsorbent mass of 0.030 g, adsorption contact time of 45 min and initial concentration of paracetamol

at 16 ppm with optimum adsorption capacity of 14.3396 mg/g. The adsorption kinetics model used for paracetamol adsorption by nanoparticles follows the pseudo-second-order kinetic model or the Ho-McKay model, with an adsorption rate constant value of $0.0324 \text{ g mg}^{-1} \text{ min}^{-1}$, and the adsorption process occurs follows the Dubinin-Radushkevich isotherm model with an adsorption free energy value of $707.1068 \text{ kJ mol}^{-1}$, this value indicates the adsorption process occurs chemically or chemisorption.

■ AUTHOR CONTRIBUTIONS

Nurmala served as researcher, data collector, writer, conducting revisions. Adhitasari Suratman as correspondent writer, research supervisor, checks revision results, provides suggestions for improvements, final assessment of the data and written reports and Suherman served as research supervisor, checks revision results, and provides suggestions for improvements to data and written reports.

■ REFERENCES

- [1] Vinayagam, V., Murugan, S., Kumaresan, R., Narayanan, M., Sillanpää, M., Viet N Vo, D., Kushwaha, O.S., Jenis, P., Potdar, P., and Gadiya, S., 2022, Sustainable adsorbents for the removal of pharmaceuticals from wastewater: A review, *Chemosphere*, 300, 134597.
- [2] Dhiman, N., and Sharma, N., 2019, Removal of pharmaceutical drugs from binary mixtures by use of ZnO nanoparticles: (Competitive adsorption of drugs), *Environ. Technol. Innovation*, 15, 100392.
- [3] Bernal, V., Giraldo, L., and Moreno-Piraján, J.C., 2021, Understanding the solid- liquid equilibria between paracetamol and activated carbon: Thermodynamic approach of the interactions adsorbent-adsorbate using equilibrium, kinetic and calorimetry data, *J. Hazard. Mater.*, 419, 126432.
- [4] Amouzgar, P., Vakili, M., Chan, E.S., and Salamatinia, B., 2017, Effects of beading parameters for development of chitosan-nano-activated carbon biocomposite for acetaminophen elimination from aqueous sources, *Environ. Eng. Sci.*, 34 (11), 805–815.
- [5] Koagouw, W., Arifin, Z., Olivier, G.W.J., and Ciocan, C., 2021, High concentrations of paracetamol in effluent dominated waters of Jakarta Bay, Indonesia, *Mar. Pollut. Bull.*, 169, 112558.
- [6] Mashayekh-Salehi, A., and Moussavi, G., 2015, Removal of acetaminophen from the contaminated water using adsorption onto carbon activated with NH_4Cl , *Desalin. Water Treat.*, 57 (27), 12861–12873.
- [7] Igwegbe, C.A., Aniagor, C.O., Oba, S.N., Yap, P.S., Iwuchukwu, F.U., Liu, T., de Souza, E.C., and Ighalo, J.O., 2021, Environmental protection by the adsorptive elimination of acetaminophen from water: A comprehensive review, *J. Ind. Eng. Chem.*, 104, 117–135.
- [8] Shokry, A., El Tahan, A., Ibrahim, H., Soliman, M., and Ebrahim, S., 2019, Polyaniline/akaganéite superparamagnetic nanocomposite for cadmium uptake from polluted water, *Desalin. Water Treat.*, 171, 205–215.
- [9] Liakos, E.V., Lazaridou, M., Michailidou, G., Koumentakou, I., Lambropoulou, D.A., Bikiaris, D.N., and Kyzas, G.Z., 2021, Chitosan adsorbent derivatives for pharmaceuticals removal from effluents: A review, *Macromol*, 1 (2), 130–154.
- [10] Zekić, E., Vuković, Ž., and Halkijević, I., 2018, Application of nanotechnology in wastewater treatment, *Grđevinar*, 70 (4), 315–323.
- [11] Niculescu, A.G., and Grumezescu, A.M., 2022, Applications of chitosan-alginate-based nanoparticles—An up-to-date review, *Nanomaterials*, 12 (2), 186.
- [12] Ferrah, N., Merghache, D., Meftah, S., and Benbellil, S., 2022, A new alternative of a green polymeric matrix chitosan/alginate-polyethylenimine-thylene phosphonic acid for pharmaceutical residues adsorption, *Environ. Sci. Pollut. Res.*, 29 (9), 13675–13687.
- [13] Zhou, Z., Lin, S., Yue, T., and Lee, T.C., 2014, Adsorption of food dyes from aqueous solution by glutaraldehyde cross-linked magnetic chitosan nanoparticles, *J. Food Eng.*, 126, 133–141.
- [14] Kyzas, G.Z., Kostoglou, M., Lazaridis, N.K.,

- Lambropoulou, D.A., and Bikiaris, D.N., 2013, Environmental friendly technology for the removal of pharmaceutical contaminants from wastewaters using modified chitosan adsorbents, *Chem. Eng. J.*, 222, 248–258.
- [15] Al-Ogaidi, I., 2018, Evaluation of the antioxidant and anticancer effects of biodegradable/biocompatible chitosan–alginate nanoparticles loaded with vitamin C, *Int. J. Pharm. Res. Allied Sci.*, 7 (3), 189–197.
- [16] Karthikeyan, P., Banu, H.A.T., and Meenakshi, S., 2019, Synthesis and characterization of metal loaded chitosan–alginate biopolymeric hybrid beads for the efficient removal of phosphate and nitrate ions from aqueous solution, *Int. J. Biol. Macromol.*, 130, 407–418.
- [17] Kulig, D., Zimoch-Korzycka, A., Jarmoluk, A., and Marycz, K., 2016, Study on alginate–chitosan complex formed with different polymers ratio, *Polymers*, 8 (5), 167.
- [18] Kunjumon, R., Viswanathan, G., and Baby, S., 2021, Biocompatible madecassoside encapsulated alginate chitosan nanoparticles, their anti-proliferative activity on C6 glioma cells, *Carbohydr. Polym. Technol. Appl.*, 2, 100106.
- [19] Shaheen, T.I., Montaser, A.S., and Li, S., 2019, Effect of cellulose nanocrystals on scaffolds comprising chitosan, alginate and hydroxyapatite for bone tissue engineering, *Int. J. Biol. Macromol.*, 121, 814–821.
- [20] Othayoth, R., Mathi, P., Bheemanapally, K., Kakarla, L., and Botlagunta, M., 2015, Characterization of vitamin–cisplatin-loaded chitosan nanoparticles for chemoprevention and cancer fatigue, *J. Microencapsulation*, 32 (6), 578–588.
- [21] Shamszadeh, S., Akrami, M., and Asgary, S., 2022, Size-dependent bioactivity of electrosprayed core–shell chitosan–alginate particles for protein delivery, *Sci. Rep.*, 12 (1), 20097.
- [22] Galan, J., Trilleras, J., Zapata, P.A., Arana, V.A., and Grande-Tovar, C.D., 2021, Optimization of chitosan glutaraldehyde-crosslinked beads for reactive blue 4 anionic dye removal using a surface response methodology, *Life*, 11 (2), 85.
- [23] Ramli, R.H., Soon, C.F., and Mohd Rus, A.Z., 2016, Synthesis of chitosan/alginate/silver nanoparticles hydrogel scaffold, *MATEC Web Conf.*, 78, 01031.
- [24] Islam, N., Wang, H., Maqbool, F., and Ferro, V., 2019, *In vitro* enzymatic digestibility of glutaraldehyde-crosslinked chitosan nanoparticles in lysozyme solution and their applicability in pulmonary drug delivery, *Molecules*, 24 (7), 1271.
- [25] Liakos, E.V., Lazaridou, M., Michailidou, G., Koumentakou, I., Lambropoulou, D.A., Bikiaris, D.N., and Kyzas, G.Z., 2021, Chitosan adsorbent derivatives for pharmaceuticals removal from effluents: A review, *Macromol*, 1 (2), 130–154.
- [26] Spaltro, A., Pila, M.N., Colasurdo, D.D., Nosedo Grau, E., Román, G., Simonetti, S., and Ruiz, D.L., 2021, Removal of paracetamol from aqueous solution by activated carbon and silica. experimental and computational study, *J. Contam. Hydrol.*, 236, 103739.
- [27] Rahdar, S., Taghavi, M., Khaksefidi, R., and Ahmadi, S., 2019, Adsorption of arsenic(V) from aqueous solution using modified saxaul ash: isotherm and thermodynamic study, *Appl. Water Sci.*, 9 (4), 87.
- [28] Rezaei, H., Haghshenasfard, M., and Moheb, A., 2017, Optimization of dye adsorption using Fe₃O₄ nanoparticles encapsulated with alginate beads by Taguchi method, *Adsorpt. Sci. Technol.*, 35 (1-2), 55–71.
- [29] Chakraborty, R., Asthana, A., Singh, A.K., Jain, B., and Susan, A.B.H., 2022, Adsorption of heavy metal ions by various low-cost adsorbents: A review, *Int. J. Environ. Anal. Chem.*, 102 (2), 342–379.
- [30] Sahoo, T.R., and Prelot, B., 2020, “Adsorption processes for the removal of contaminants from wastewater: The perspective role of nanomaterials and nanotechnology” in *Nanomaterials for the Detection and Removal of Wastewater Pollutants*, Eds. Bonelli, B., Freyria, F.S., Rossetti, I., and Sethi, R., Elsevier, Amsterdam, Netherlands, 161–222.
- [31] Sun, Z., Qu, K., Cheng, Y., You, Y., Huang, Z., Umar, A., Ibrahim, Y.S., Algadi, H., Castañeda, L.,

- Colorado, H.A., and Guo, Z., 2021, Corncob-derived activated carbon for efficient adsorption dye in sewage, *ES Food Agrofor.*, 4, 61–73.
- [32] Piccin, J.S., Dotto, G.L., and Pinto, L.A.A., 2011, Adsorption isotherms and thermochemical data of FD&C red N 40 binding by chitosan, *Braz. J. Chem. Eng.*, 28 (2), 295–304.
- [33] Iryani, A., Ilmi, M.M., and Hartanto, D., 2017, Adsorption study of Congo red dye with ZSM-5 directly synthesized from Bangka kaolin without organic template, *Malays. J. Fundam. Appl. Sci.*, 13 (4), 832–839.